



Heterogeneous selective oxidation catalysts based on coordination polymer MIL-101 and transition metal-substituted polyoxometalates

N.V. Maksimchuk^a, M.N. Timofeeva^a, M.S. Melgunov^a, A.N. Shmakov^a, Yu.A. Chesalov^a, D.N. Dybtsev^b, V.P. Fedin^b, O.A. Kholdeeva^{a,*}

^a Boreskov Institute of Catalysis, Prospekt Akademika Lavrentieva 5, Novosibirsk 630090, Russia

^b Nikolaev Institute of Inorganic Chemistry, Prospekt Akademika Lavrentieva 3, Novosibirsk 630090, Russia

ARTICLE INFO

Article history:

Received 4 October 2007

Revised 23 March 2008

Accepted 11 May 2008

Available online 12 June 2008

Keywords:

Metal-organic framework

MIL-101

Supported polyoxometalate

Composite materials

Co(II)

Ti(IV)

Selective oxidation

Alkene

Molecular oxygen

Hydrogen peroxide

ABSTRACT

Titanium- and cobalt-monosubstituted Keggin heteropolyanions, $[\text{PW}_{11}\text{CoO}_{39}]^{5-}$ and $[\text{PW}_{11}\text{TiO}_{40}]^{5-}$, were electrostatically bound to the chromium terephthalate polymer matrix MIL-101. The MIL-supported polyoxometalate (POM) catalysts were characterized by elemental analysis, XRD, N_2 adsorption, and FT-IR-spectroscopy. The catalytic performance of both MIL-101 and the novel composite materials M-POM/MIL-101 was assessed in the oxidation of three representative alkenes— α -pinene, caryophyllene, and cyclohexene—using molecular oxygen and aqueous hydrogen peroxide as oxidants. Ti-POM/MIL-101 demonstrated fairly good catalytic activity and selectivity in α -pinene allylic oxidation and caryophyllene epoxidation with hydrogen peroxide, whereas Co-POM/MIL-101 catalyzed α -pinene allylic oxidation by molecular oxygen. Both composite materials are stable to POM leaching, behave as true heterogeneous catalysts, and can be used repeatedly without sustaining a loss of activity and selectivity in oxidations with O_2 and H_2O_2 , provided that rather mild reaction conditions ($T < 50^\circ\text{C}$, $[\text{H}_2\text{O}_2] < 0.2\text{ M}$) are used with the latter oxidant.

© 2008 Elsevier Inc. All rights reserved.

1. Introduction

The design of active, selective, and recyclable heterogeneous catalysts is a challenging goal of oxidation catalysis. Most known solid catalysts, including redox molecular sieves, encapsulated, grafted, and tethered redox metal complexes, suffers from leaching of the active metal while using them in liquid-phase selective oxidation processes and, in effect, behave as homogeneous rather than heterogeneous catalysts [1–3]. A rare example of a highly efficient and true heterogeneous catalyst is the microporous titanium silicalite TS-1 developed by Enichem, which is currently used in three industrial processes for selective oxidation of small organic substrates, specifically phenol, cyclohexanone, and propene [4,5]. Many research efforts are directed toward synthesis of mesoporous M,Si-catalysts, but most of them undergo irreversible deactivation in the liquid phase due to hydrolysis, oligomerization, and subsequent leaching of the active metal.

Transition-metal oxoanion nanosized clusters or polyoxometalates (POMs) have received increasing attention as oxidation catalysts because of their numerous advantageous properties, such

as inorganic nature, thermodynamic stability to oxidation, hydrostability, tunability of redox and acid properties, and so on [6–18]. Transition metal monosubstituted POMs (M-POMs) are useful single-site catalysts where active metal M is isolated in and strongly bound to an inorganic metal-oxide matrix and thus is prevented from oligomerization and leaching [19,20]. Much work is directed to immobilization of POMs on various solid supports via dative [21], covalent [22], or electrostatic [23–28] binding.

Recently, Férey and co-workers have demonstrated a successful immobilization of a Keggin heteropolytungstate within the cages of the nanoporous metal-organic framework MIL-101, which has a rigid zeotype crystal structure, large pores, and outstanding surface area and also is resistant to air, water, common solvents, and thermal treatment [29]. To date, no examples of catalysis over POM/MIL-101 composite materials have been presented.

Here we report on the preparation of novel heterogeneous catalysts, based on MIL-101 and catalytically active Co- and Ti-monosubstituted Keggin-type heteropolyanions, $[\text{PW}_{11}\text{CoO}_{39}]^{5-}$ and $[\text{PW}_{11}\text{TiO}_{40}]^{5-}$, incorporated within the coordination polymer nanocages. We describe their catalytic performance in liquid-phase oxidation of three representative alkenes—cyclohexene, α -pinene, and caryophyllene—using green oxidants— O_2 and H_2O_2 .

α -Pinene is the main component of gum turpentine, whereas caryophyllene is a constituent of some essential oils (e.g., clove oil).

* Corresponding author. Fax: +7 383 330 95 73.

E-mail address: khold@catalysis.nsk.su (O.A. Kholdeeva).

Both are low-cost and readily available renewable raw materials for the production of a wide variety of fine chemicals, such as fragrances, flavors, drugs, and agrochemicals [30–32]. Caryophyllene oxide has received FDA approval as a food and cosmetic stabilizer [33]. It is also used as a flavoring substance, along with the α -pinene allylic oxidation products verbenol and verbenone [31].

2. Experimental

2.1. Materials

α -Pinene, containing 98% of α -pinene and 2% of β -pinene, was obtained by vacuum rectification of gum turpentine. Hydrogen peroxide was used as 30% solution in water; its precise concentration was determined iodometrically before use. All other reactants were obtained commercially and used without further purification.

Acid sodium salt $\text{NaH}_3[\text{PW}_{11}\text{Ti}(\text{OH})\text{O}_{39}]$ ($\text{NaH}_4\text{PW}_{11}\text{TiO}_{40}$, Ti-POM) was synthesized as described previously [34]. Tetrabutylammonium (TBA) salt $[\text{Bu}_4\text{N}]_4\text{H}[\text{PW}_{11}\text{Co}(\text{H}_2\text{O})\text{O}_{39}]$ (Co-POM) was prepared by metathesis of $\text{Na}_5\text{PW}_{11}\text{CoO}_{39}$ with TBABr in water at pH 2.7 as described previously [26]. The presence of one acid proton in Co-POM was confirmed by potentiometric titration with methanolic TBAOH (Aldrich).

2.2. Catalyst preparation and characterization

2.2.1. MIL-101 synthesis

The coordination polymer MIL-101 was prepared as described by Férey et al. [29]. In a typical synthesis, a mixture of 1.2 g (3 mmol) of $\text{Cr}(\text{NO}_3)_3 \cdot 9\text{H}_2\text{O}$, 500 mg of terephthalic acid (H_2bdc , 3 mmol), and 0.6 mL of 5 M HF (3 mmol) in 15 mL H_2O was heated at 220 °C for 8 h in a Teflon-lined stainless steel bomb. The resulting green solid was passed through a coarse glass filter to remove the unreacted colorless crystals of H_2bdc and then filtered on the dense paper filter. Then the green raw product was washed in hot DMF (100 °C, 8 h, 2 times) and in hot EtOH (80 °C, 8 h, 2 times), filtered off, and dried overnight in an oven at 75 °C.

2.2.2. Immobilization of M-POMs on MIL-101

Adsorption measurements were carried out in a glass reactor at 25 °C. The adsorbent (MIL-101, 40 mg) was placed into the reactor, and a solution of Ti-POM in acetonitrile (1 mL, 1–10 mmol/L) was added. Samples of the solution were obtained by a syringe (100 μL) after 24 h and diluted with water (50 mL). Then the Ti-POM concentration in solution was determined by UV–vis ($\lambda = 250 \text{ nm}$).

Desorption measurements were carried out at 25 °C as follows. MeCN (0.5 mL) was added to 40 mg of a MIL-101 sample containing Ti-POM (with the amount of Ti-POM determined from the adsorption measurements). Samples of the solution (100 μL) were obtained by a syringe after 24 h and diluted with water (50 mL); then the Ti-POM concentration in the solution was determined by UV–vis. The amount of POM irreversibly adsorbed on MIL-101 was determined from the point at which the desorption curve cut the axis (Y). A similar procedure was used for the adsorption/desorption measurements for Co-POM.

Supported M-POM/MIL-101 samples were prepared by dissolving 11 mg of M-POM ($\text{NaH}_4\text{PW}_{11}\text{TiO}_{40}$ or $\text{TBA}_4\text{HPW}_{11}\text{CoO}_{39}$) in MeCN (1.5 mL), adding 100 mg of MIL-101, stirring for 3 h, storing overnight at room temperature, filtering off, washing with MeCN, and then drying in air until the weight remained constant. The complete disappearance of M-POM in the MeCN solution was confirmed by UV–vis. The M-POM loading also was evaluated by the elemental analysis.

The textural characteristics of the supported catalysts were determined from nitrogen adsorption isotherms. The specific surface area and pore volume were measured by the comparative

method [35]. The catalysts also were characterized by XRD and FT-IR spectroscopy.

2.3. Catalytic oxidation

Catalytic experiments were carried out in thermostatted glass vessels under vigorous stirring at 50 °C for α -pinene oxidation with molecular oxygen and caryophyllene oxidation with H_2O_2 , at 30 °C for α -pinene oxidation with H_2O_2 , and at 70 °C for cyclohexene oxidation with H_2O_2 . Typically, the reactions of alkene oxidation with H_2O_2 were initiated by adding H_2O_2 (0.12 mmol for α -pinene, 0.10 mmol for caryophyllene, and 0.40 mmol for cyclohexene oxidation) to a mixture containing an organic substrate (0.1 mmol of α -pinene or caryophyllene, or 0.2 mmol of cyclohexene), 14 mg of the catalyst (6×10^{-4} mmol of Ti-POM), an internal standard (biphenyl), and 1 mL of acetonitrile.

In α -pinene oxidation with molecular oxygen, 0.1 mmol of α -pinene was added to a preliminary blown with dioxygen mixture, which contained 14 mg of the catalyst (4×10^{-4} mmol of Co-POM), internal standard (biphenyl), and 1 mL of acetonitrile. Aliquots of the reaction mixture were withdrawn periodically during the reaction course by a syringe through a septum. Each experiment was reproduced at least 2 or 3 times. The reaction products were identified by GC-MS and quantified by GC. After the reactions, catalysts were filtered off, washed with acetonitrile, dried in air at room temperature overnight, and then reused.

2.4. Instrumentation

GC analyses were performed using a Tsvet-500 gas chromatograph equipped with a flame ionization detector and a Supelco MDN-5S quartz capillary column (30 m \times 0.25 mm). GC-MS analyses were carried out using an Agilent 6890 gas chromatograph (with an HP-5ms 30 m \times 0.25 mm quartz capillary column) equipped with an Agilent MSD 5973 quadrupole mass-selective detector. FT-IR spectra were recorded using KBr pellets containing 0.3 wt% of sample on a BOMEM-MB-102 spectrometer in the 250–4000 cm^{-1} range. Nitrogen adsorption at 77 K was studied using an ASAP-2020 instrument within a partial pressure range of 10^{-6} –1.0. Before measurements, the samples were degassed at 90 °C for 48 h. UV–vis spectra were recorded using a Specord M40 spectrophotometer ($l = 10 \text{ mm}$, accuracy of measurements $\pm 10\%$). Particle size was measured using a Shimadzu SALD-2101 laser diffraction particle size analyzer. XRD measurements were performed on a high-precision X-ray diffractometer mounted on beamline 2 of the VEPP-3 storage ring at the Siberian Synchrotron Radiation Center (SSRC). The radiation wavelength was $\lambda = 0.15393 \text{ nm}$. The high natural collimation of synchrotron radiation beam, flat perfect crystal analyzer, and parallel Soller slit on the diffracted beam provided very high instrumental resolution of the diffractometer in a small-angle region of $2\theta = 0.5^\circ$ – 10° and higher.

3. Results and discussion

3.1. Catalysts preparation and characterization

MIL-101 was prepared as described by Férey et al. [29]. The XRD data confirm the MIL-101 structure reported in [29]. The XRD pattern calculated for MIL-101 based on the structural information (Fig. 1A) and the experimental XRD pattern (Fig. 1B) were very close. The size of the MIL-101 particles was in the range of 5–10 μm ; such small particle sizes suggests no significant diffusion limitations inside the MIL-101 crystals.

Co-POM/MIL-101 and Ti-POM/MIL-101 composites (shown schematically in Fig. 2) were prepared by M-POM adsorption from

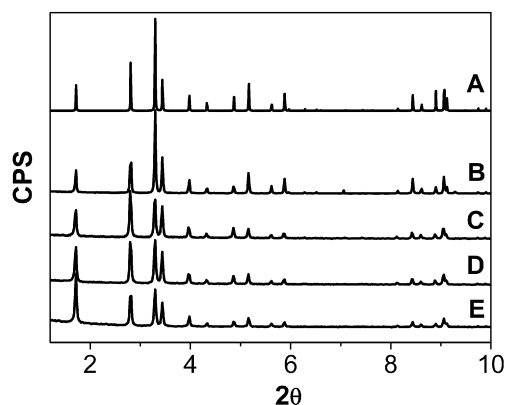


Fig. 1. Calculated XRD pattern for MIL-101 based on the structural information (A) and experimental XRD patterns for MIL-101 (B), Ti-POM/MIL-101 (C), Co-POM/MIL-101 (D), and Co-POM/MIL-101 after five cycles of α -pinene oxidation with molecular oxygen (E).

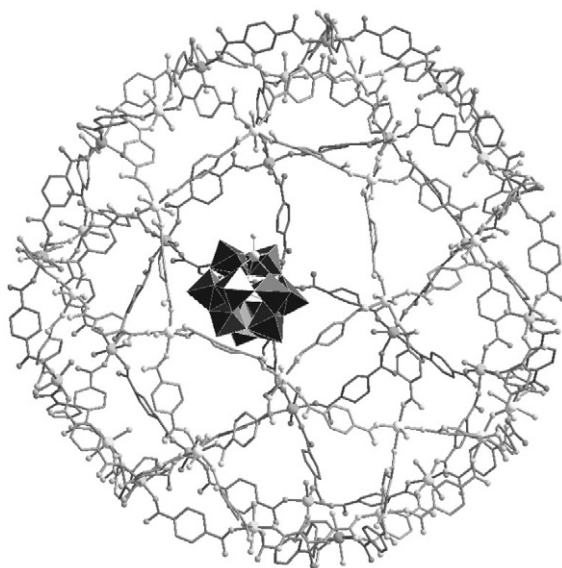


Fig. 2. Schematic representation of M-POM encapsulated within MIL-101 matrix.

acetonitrile solutions at 25 °C. The adsorption/desorption processes were monitored by UV–vis (see Section 2 for details). The adsorption and desorption curves for $\text{NaH}_4\text{PW}_{11}\text{TiO}_{40}$ and $[\text{Bu}_4\text{N}]_4\text{HPW}_{11}\text{CoO}_{39}$ are shown in Figs. 3a and 3b, respectively. An irreversible character of the sorption of about 10 wt% of $\text{PW}_{11}\text{TiO}_{40}^{5-}$ or 7 wt% of $\text{PW}_{11}\text{CoO}_{39}^{5-}$ (~ 1 POM anion per MIL-101 nanocage) indicated a strong interaction between POM and the support. The immobilized POM could be reextracted using a

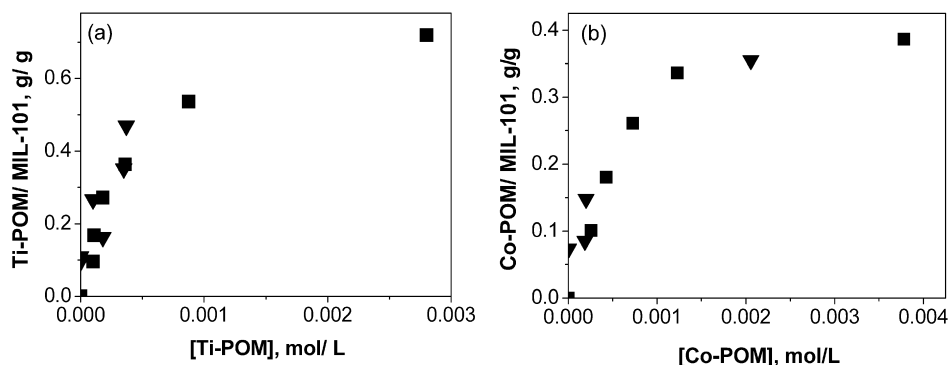


Fig. 3. Adsorption/desorption isotherms for (a) $\text{NaH}_4\text{PW}_{11}\text{TiO}_{40}$ and (b) $[\text{Bu}_4\text{N}]_4\text{HPW}_{11}\text{CoO}_{39}$ on MIL-101 (MeCN, 25 °C). Adsorption and desorption curves are marked by (■) and (▼), respectively.

Table 1
Physico-chemical properties of the catalysts studied

Sample	M/W/Cr ^a (wt%)	M/W/Cr ^b (wt%)	A ^c (m ² /g)	V _p ^d (cm ³ /g)
MIL-101	–	–	2220 25 ^e , 80 ^f	1.13 0 ^{e,f}
10% Ti-POM/MIL-101	0.17/7.4/12.0	0.13/4.1/12.1 0.14/5.1/14.4 ^g	1930	0.96
7% Co-POM/MIL-101	0.14/5.2/12.4	0.14/4.15/15.1 0.14/4.2/14.8 ^h	2050 1610 ⁱ	1.03 0.81 ⁱ

^a Evaluated from the adsorption data.

^b Based on the elemental analysis data.

^c Specific surface area.

^d Mesopore volume.

^e After three treatments with 0.4 M H₂O₂ at 70 °C for 6 h.

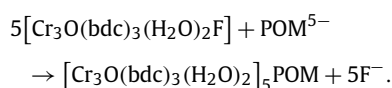
^f After four treatments with 0.1 M H₂O₂ at 70 °C for 6 h.

^g After five treatments with 0.2 M H₂O₂ at 50 °C for 4 h.

^h After three catalytic cycles of α -pinene oxidation with molecular oxygen, the reaction conditions as in Table 2.

ⁱ After five catalytic cycles of α -pinene oxidation with molecular oxygen, the reaction conditions as in Table 2.

1 M solution of Bu_4NClO_4 in MeCN, demonstrating the electrostatic character of binding between POM anion and the positively charged surface of the MIL-101 nanocage,



Some redistribution of XRD reflexes intensities was observed for the Co-POM/MIL-101 and Ti-POM/MIL-101 composites compared with the initial MIL-101 support (Fig. 1). A similar redistribution was reported for POM-modified MIL-101 by Férey [29] and attributed to interaction of POM anion with MIL-101 surface; however, both the positions and width of the X-ray reflections remained unchanged compared with the initial MIL-101 sample. Thus, the composite materials obtained did not lose their crystalline structure during impregnation with POM. This was also confirmed by the FT-IR study (*vide infra*)

Table 1 gives the elemental analysis data for the supported POM/MIL-101 samples along with the M/W/Cr values calculated for a specific POM loading acquired from the adsorption measurements. Keeping in mind that elemental analysis of POMs in the presence of MIL is not an easy task, we may conclude that the amount of POM in the composite materials obtained by the two methods were quite similar.

Table 1 also presents the textural properties (i.e., specific surface areas and mesopore volumes) acquired from the low-temperature N₂ adsorption measurements. Fig. 4a shows N₂ adsorption isotherms for both MIL-101 and supported POMs in semilogarithmic coordinates. The isotherms are characterized by

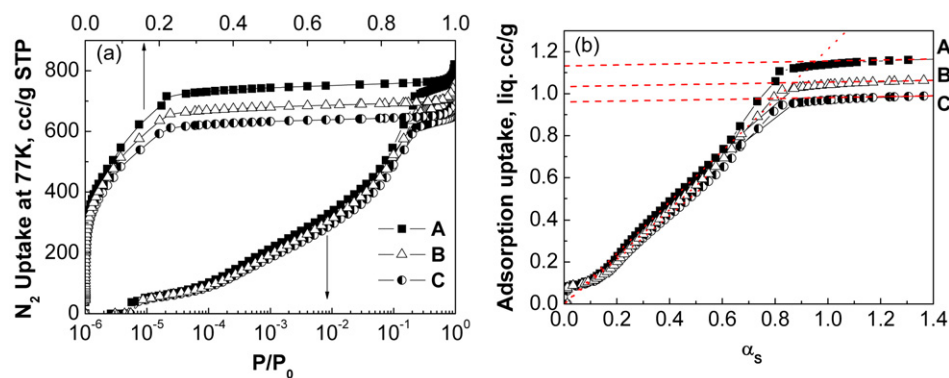


Fig. 4. (a) N₂ adsorption isotherms and (b) adsorption isotherms in α_s coordinates for MIL-101 (A), Co-POM/MIL-101 (B), and Ti-POM/MIL-101 (C).

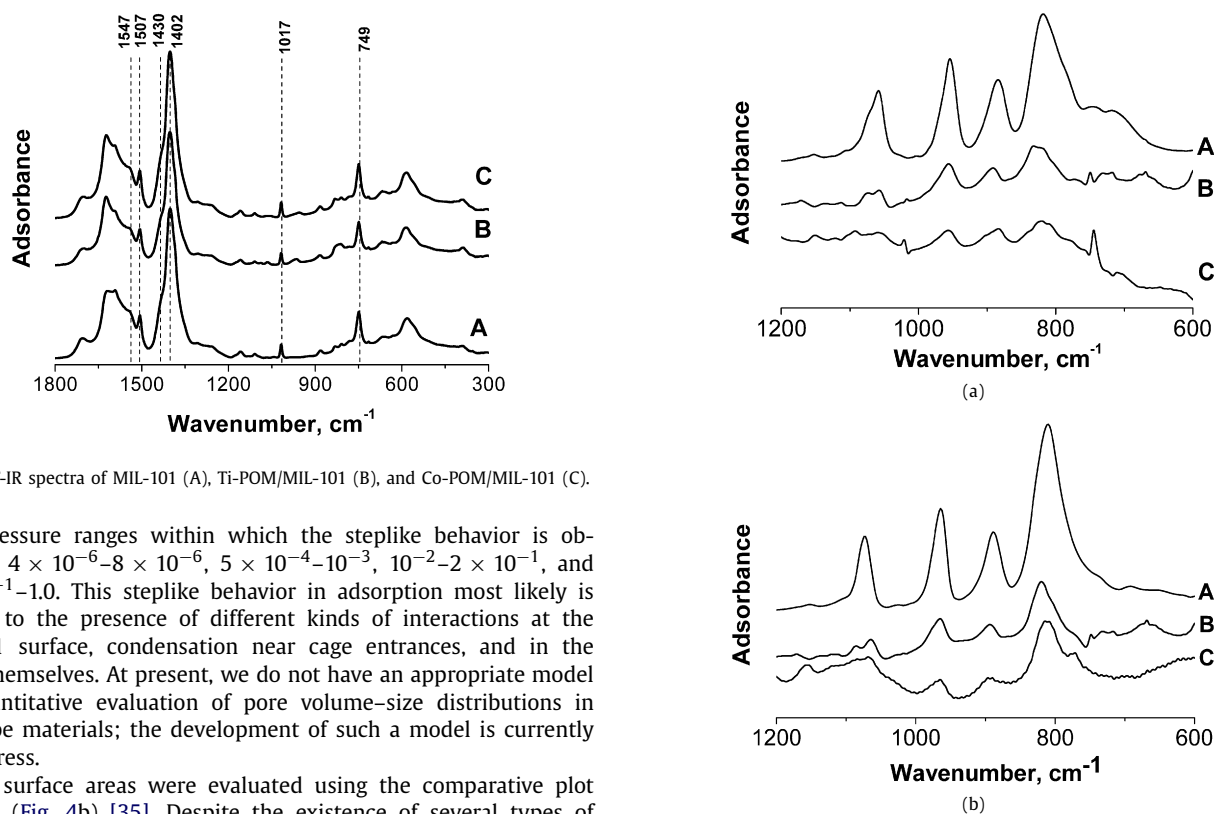


Fig. 5. FT-IR spectra of MIL-101 (A), Ti-POM/MIL-101 (B), and Co-POM/MIL-101 (C).

four pressure ranges within which the steplike behavior is observed: 4×10^{-6} – 8×10^{-6} , 5×10^{-4} – 10^{-3} , 10^{-2} – 2×10^{-1} , and 7×10^{-1} – 1.0 . This steplike behavior in adsorption most likely is related to the presence of different kinds of interactions at the MIL-101 surface, condensation near cage entrances, and in the cages themselves. At present, we do not have an appropriate model for quantitative evaluation of pore volume–size distributions in MIL-type materials; the development of such a model is currently in progress.

The surface areas were evaluated using the comparative plot method (Fig. 4b) [35]. Despite the existence of several types of pores, the comparative plots demonstrated a linear behavior in the range of almost complete monolayer formation ($0.1 < \alpha_s < 0.4$). The corresponding interpolation lines passed through the origin, indicating the essential nonmicroporous nature of the materials studied. The observed affinity of the reference and study materials provides strong evidence of the correctness of the surface area measurements. Of note, determining surface area by means of BET or Langmuir interpolation is not reliable, because some points on adsorption isotherms (which comprise both layered adsorption and condensation) can be included in the interpolation. The second linear range was observed for α_s near 2.0. The corresponding slope gave the surface area outside the structural mesopores, and the intercept on the ordinate axis gave the volume of mesopores. The measured surface areas and volume of pores are shown in Table 1. The volume of mesopores for initial MIL-101 was close to the theoretical approximation of 1.37 cm³/g. The decreased pore volume on POM deposition corresponds to the mass increase due to the introduction of POM (Table 1).

FT-IR studies were performed to check whether the M-POM and MIL structures were preserved in the composite materials. FT-IR spectra of MIL-101, Ti-POM/MIL-101, and Co-POM/MIL-101 are pre-

Fig. 6. FT-IR spectra of (a) Co-POM and (b) Ti-POM: M-POM (A), M-POM/MIL-101 (B), and M-POM/MIL-101 after 4 catalytic cycles of α-pinene oxidation (C). (B) and (C)—after subtraction of the spectrum of MIL-101.

sented in Fig. 5. These spectra look quite similar because of the rather low POM loading; the most intense peaks belong to the MIL-101 matrix. Strong bands in the region of 1800–1300 cm⁻¹ correspond to ν_{as}(COO), ν_s(COO), and ν(C–C) vibrations, implying the presence of dicarboxylate linker in the MIL framework. Rather weak and narrow bands at 1017 and 749 cm⁻¹ can be attributed to δ(C–H) and γ(C–H) vibrations of aromatic rings, respectively. Weak bands in the spectral region of 700–400 cm⁻¹ are most likely due to in-plane and out-of-plane bending modes of COO-groups [36].

Fig. 6 shows the IR spectra of bulk M-POMs and of the MIL-supported M-POMs after subtraction of the spectrum of MIL-101. The IR spectra of the M-POM/MIL composites exhibit the principal stretching modes of the Keggin POM unit: 1077 and 1073 ν_{as}(PO₄); 950 and 969 ν_{as}(W=O); and 883, 823, and 890, and 803 cm⁻¹ ν_{as}(W–O–W), for Co-POM and Ti-POM, respectively. This definitely indicates that the heteropolyanion structure was maintained after immobilization.

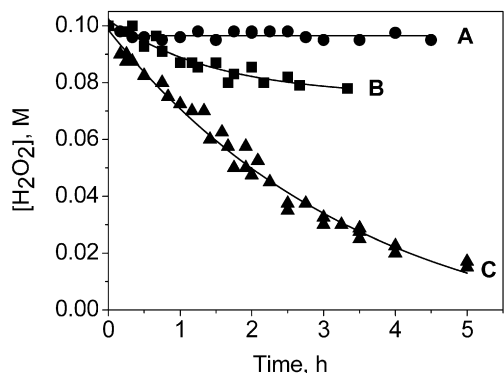


Fig. 7. Hydrogen peroxide decomposition: (A) blank experiment at 50 °C, (B) over MIL-101 at 30 °C, and (C) over MIL-101 at 50 °C.

3.2. Catalytic oxidations

The catalytic performance of the new M-POM/MIL-101 composites was assessed in α -pinene oxidation with H₂O₂ and O₂, as well as in cyclohexene and caryophyllene oxidation with H₂O₂ in acetonitrile (see Scheme 1).

Table 2 presents the results of the alkene oxidations over Ti- and Co-POM/MIL-101 catalysts, along with blank experiments and experiments performed in the presence of the corresponding homogeneous M-POMs. The catalytic study revealed that both Ti- and Co-POM incorporated into MIL-101 matrix catalyzed alkene oxidation with H₂O₂ and O₂, respectively, whereas the matrix alone was quite inert in most cases (Table 2). The MIL matrix exhibited some activity only in caryophyllene oxidation with H₂O₂, in contrast with α -pinene oxidation with H₂O₂, where the matrix was almost inert. This may be due to the higher reaction temperature used for the caryophyllene oxidation. Indeed, no H₂O₂ decomposition over MIL-101 occurred at 30 °C, whereas some activity of the matrix was observed at 50 °C (Fig. 7).

It is noteworthy that the activity of the M-POM/MIL catalysts expressed in TOF values determined from the initial rates of substrate consumption was close to the activity of the corresponding homogeneous M-POMs; this indicates that the activity did not de-

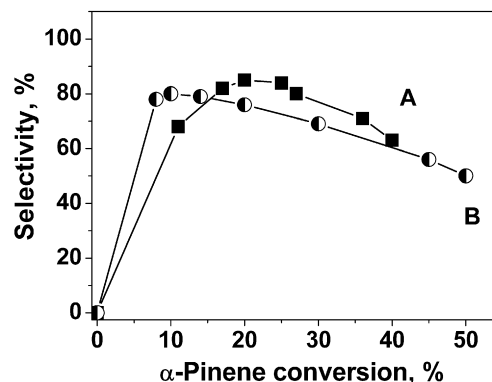
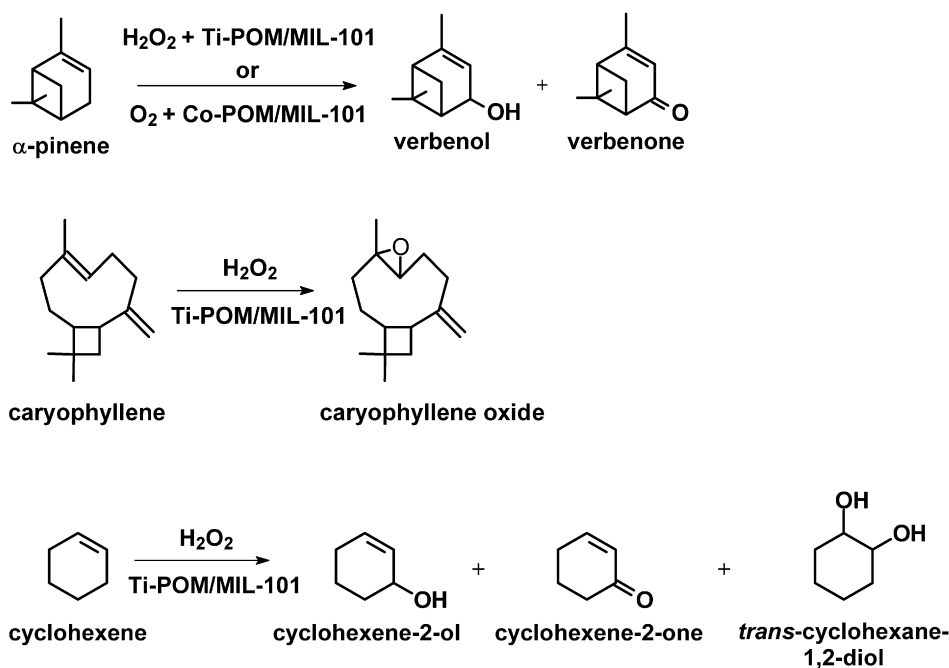


Fig. 8. Effect of α -pinene conversion on verbenol/verbenone selectivity in oxidation with (A) H₂O₂ over Ti-POM/MIL-101 and (B) O₂ over Co-POM/MIL-101.

cline on immobilization of POMs. In both catalytic systems studied, α -pinene was converted mainly to the allylic oxidation products verbenol and verbenone, along with small amounts of campholenic aldehyde.

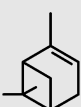
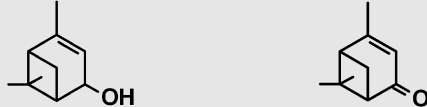
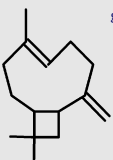
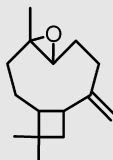
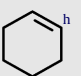
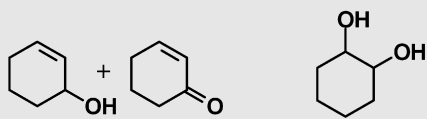
The α -pinene allylic oxidation to verbenol/verbenone with both molecular oxygen and H₂O₂ showed a strong negative effect of the reaction conversion on its selectivity due to the high reactivity of the products (Fig. 8), which is typical for allylic oxidation [37–39]. The selectivity to verbenol/verbenone reached a maximum (81–84%) at a rather low substrate conversion (15–25%) and then declined due to overoxidation processes [37–40]. Interestingly, the MIL-supported POMs were more selective in α -pinene oxidation than the silica-supported POMs [38,39], likely due to the MIL-101's zeotype porous structure and smaller pore diameter, which may have protected allylic oxidation products from further oxidative polymerization.

Oxidation of cyclohexene with H₂O₂ over Ti-POM/MIL-101 also gave predominantly the allylic oxidation products cyclohexene-2-ol and cyclohexene-2-one, pointing to a homolytic oxidation mechanism [41]. The yield of *trans*-cyclohexane-1,2-diol was lower than that of the homogeneous Ti-POM. In turn, caryophyllene oxidation with H₂O₂ over Ti-POM/MIL produced caryophyllene 4,5-



Scheme 1. Selective alkene oxidations over M-POM/MIL-101.

Table 2
Alkene oxidation with H₂O₂ and O₂ in the presence of M-POM/MIL-101 catalysts

Catalyst	Oxidant	Time (h)	Substrate conversion (%)	TOF ^a (h ⁻¹)	Selectivity ^b (%)
					
– ^d	1 atm O ₂	1	15	–	33
Co-POM ^e	1 atm O ₂	1	45	80	36
MIL-101 ^f	1 atm O ₂	2	14	–	14
Co-POM/MIL-101	1 atm O ₂	2	45	80	29
– ^d	0.12 M H ₂ O ₂	5	16	–	7
Ti-POM ^e	0.12 M H ₂ O ₂	5	42	40	25
MIL-101 ^f	0.12 M H ₂ O ₂	5	18	–	8
Ti-POM/MIL-101	0.12 M H ₂ O ₂	5	40	40	32
					
– ^d	0.1 M H ₂ O ₂	4	13	–	23
Ti-POM ^e	0.1 M H ₂ O ₂	4	60	92	52
MIL-101 ^f	0.1 M H ₂ O ₂	4	40	–	41
Ti-POM/MIL-101	0.1 M H ₂ O ₂	4	71	82	80
Ti-POM/MIL-101	0.2 M H ₂ O ₂	4	88	130	100
					
Ti-POM ^e	0.4 M H ₂ O ₂	6	7	4	7
MIL-101 ^f	0.4 M H ₂ O ₂	6	8	–	60
Ti-POM/MIL-101	0.4 M H ₂ O ₂	6	39	21	32

^a TOF = (moles of substrate consumed)/(moles of M-POM × time); determined from the initial rates.

^b GC yield based on substrate consumed (high boiling overoxidation products were also formed along with the main detectable products).

^c 0.1 M α -pinene, 14 mg catalyst (4×10^{-4} mmol of Co-POM or 6×10^{-4} mmol Ti-POM), 1 mL MeCN, 50 °C (for oxidation with O₂) or 30 °C (for oxidation with H₂O₂).

^d No catalyst was present.

^e Homogeneous catalyst (4×10^{-4} mmol of [Bu₄N]₄HPW₁₁CoO₃₉ or 6×10^{-4} mmol of NaH₄PW₁₁TiO₄₀).

^f MIL-101 matrix without M-POM.

^g 0.1 M caryophyllene, 14 mg catalyst (6×10^{-4} mmol Ti-POM), 1 mL MeCN, 50 °C.

^h 0.2 M cyclohexene, 0.4 M H₂O₂, 20 mg catalyst (9×10^{-4} mmol Ti-POM), 1.5 mL MeCN, 70 °C.

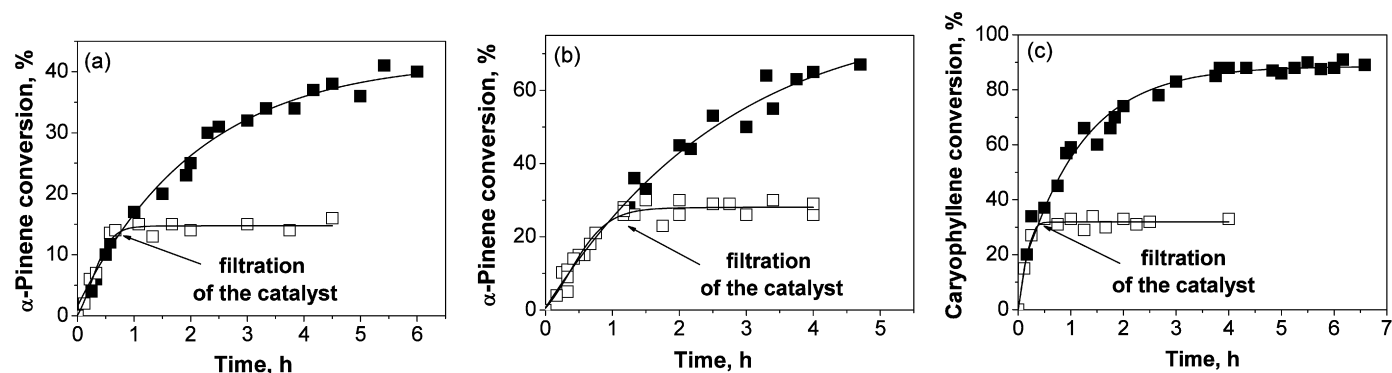


Fig. 9. Oxidation of α -pinene (a) with H₂O₂ over Ti-POM/MIL-101 and (b) with O₂ over Co-POM/MIL-101. (c) Oxidation of caryophyllene with H₂O₂ over Ti-POM/MIL-101.

monoepoxide with good to excellent selectivity. Importantly, the selectivity of caryophyllene epoxidation was significantly higher for MIL-supported Ti-POM than for homogeneous Ti-POM (Table 2). This may be due to deprotonation of the Ti-POM anion on immobilization within the MIL-101 cages via anion exchange (*vide supra*), which protected the acid-sensitive epoxide from the ring opening. The substrate conversion and epoxide selectivity increased with increasing H₂O₂ concentration (Table 2).

3.3. Catalyst stability and recycling

The essential properties of solid catalysts are the stability of the active component with respect to leaching and other transformations, and the stability of the porous structure. The nature of the catalysis is also a crucial factor in liquid-phase processes. The experiments with fast catalyst filtration performed at the reaction temperature showed no further α -pinene and caryophyllene con-

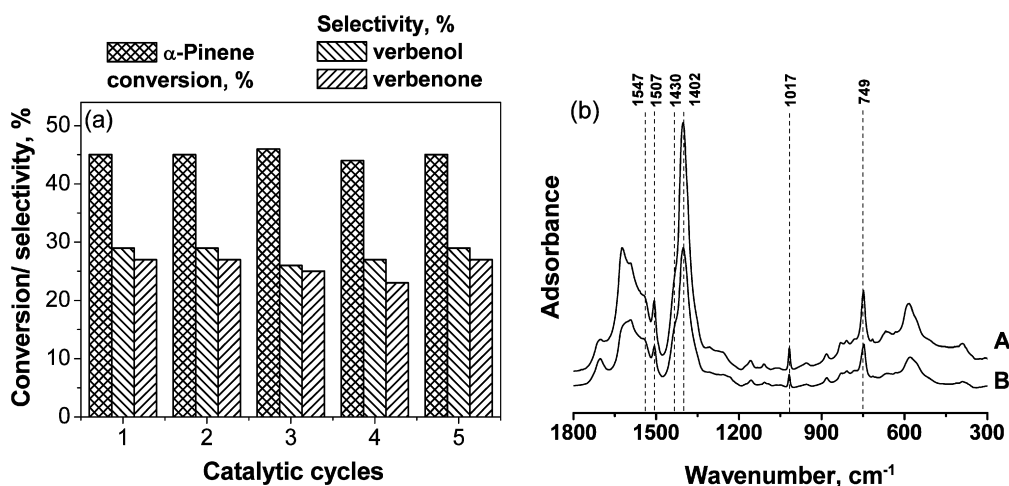


Fig. 10. (a) Co-POM/MIL-101 recycling in α -pinene oxidation with molecular oxygen and (b) FT-IR spectra of Co-POM/MIL-101: (A) initial and (B) after 5 catalytic cycles of α -pinene oxidation with O_2 .

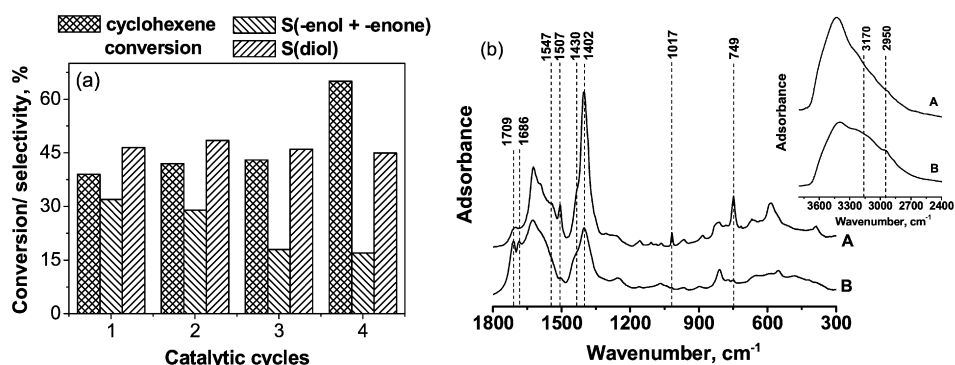


Fig. 11. (a) Ti-POM/MIL-101 recycling in cyclohexene oxidation with H_2O_2 and (b) FT-IR spectra of Ti-POM/MIL-101: (A) initial and (B) after 4 catalytic cycles of cyclohexene oxidation with H_2O_2 .

version in the filtrate after the catalysts were removed (Fig. 9). This indicates that the oxidation process is truly heterogeneous and occurs on the catalyst surface rather than in solution. Even if very small amounts of titanium or cobalt species are leached from the solid matrix during the oxidation process, the observed catalytic activity is not due to these species. Furthermore, elemental analysis data (Table 1) showed no evident POM leaching under the conditions used in this study.

An important issue that must be addressed while studying liquid-phase oxidations over a solid catalyst is a possibility of catalyst recycling. We found that the Co-POM/MIL-101 catalyst maintained its activity and selectivity for at least 5 catalytic cycles of the α -pinene oxidation with O_2 (Fig. 10a). The XRD pattern (Fig. 1D) of this catalyst demonstrated no significant changes in the structure. The N_2 adsorption measurements (Table 1) revealed a 20% decrease in the specific surface area and pore volume, which most likely can be explained by a mass increase of the catalyst with hardly removable reaction byproducts. The FT-IR study indicated preservation of both the POM and MIL-101 structures (Fig. 10b).

In contrast, when H_2O_2 was used as the oxidant, the reaction conditions had a significant impact on catalyst stability. Thus, the catalytic performance of Ti-POM/MIL-101 in cyclohexene oxidation changed significantly from cycle to cycle. After the third cycle, the catalytic activity sharply increased, and the ratio of products changed significantly, indicating that the reaction mechanism had become more heterolytic (Fig. 11a). This most likely resulted from oxidative degradation of the MIL-101 structure accompanied by Ti-POM leaching. Indeed, the FT-IR-spectra demonstrated de-

struction of the MIL-101 structure after four catalytic cycles of cyclohexene oxidation. This was manifested by decreasing intensity of the bands attributed to vibration of benzene ring at 1017 and 749 cm^{-1} and carboxylic groups of terephthalic acid in the spectral region of 1800–1300 cm^{-1} (Fig. 11b). Moreover, new bands corresponding to stretching C=O vibrations appeared at 1709 and 1686 cm^{-1} along with new stretching OH vibrations at 3300–2700 cm^{-1} , most likely indicating protonation of COO-groups [36].

In sharp contrast, the Ti-POM/MIL-101 catalyst did not lose its activity/selectivity during several catalytic cycles of both α -pinene and caryophyllene oxidation (Fig. 12). This may be explained by taking into account the milder reaction conditions used in the oxidation of these two substrates compared with the conditions for cyclohexene oxidation. Indeed, the FT-IR findings confirmed the preservation of both the POM and MIL-101 structures after catalyst recycling in α -pinene and caryophyllene oxidation with H_2O_2 (Fig. 13). In effect, after four catalytic cycles, the principal stretching modes of both the Keggin POM unit and terephthalic acid remained unchanged.

To gain insight into the factors crucial for the stability of the composite POM/MIL-101 materials, we studied the resistance of the MIL-101 matrix to aqueous H_2O_2 . Treatment of MIL-101 with H_2O_2 was followed by FT-IR, small-angle XRD, and N_2 adsorption. All of the methods collectively demonstrated the matrix was unstable at rather high oxidant concentrations (0.4 M; Table 1, Fig. 14a). After three consecutive treatments of MIL-101 with 0.1 M H_2O_2 at 70 °C, the FT-IR spectrum remained practically unchanged (Fig. 14b), but no XRD was observed. This may indicate preservation of the short-range order, but accompanied by loss of the

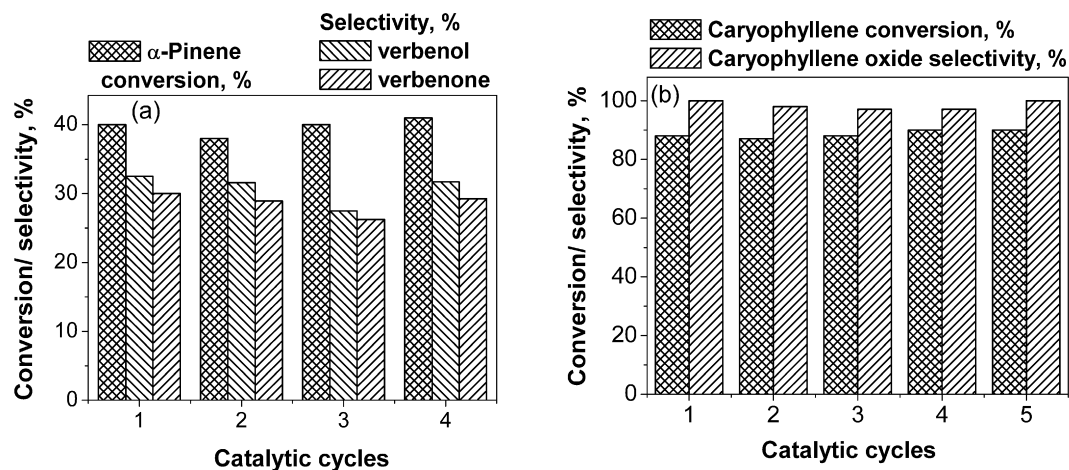


Fig. 12. Ti-POM/MIL-101 recycling in (a) α -pinene oxidation with 0.12 M H_2O_2 at 30 °C and (b) caryophyllene oxidation with 0.1 M H_2O_2 at 50 °C.

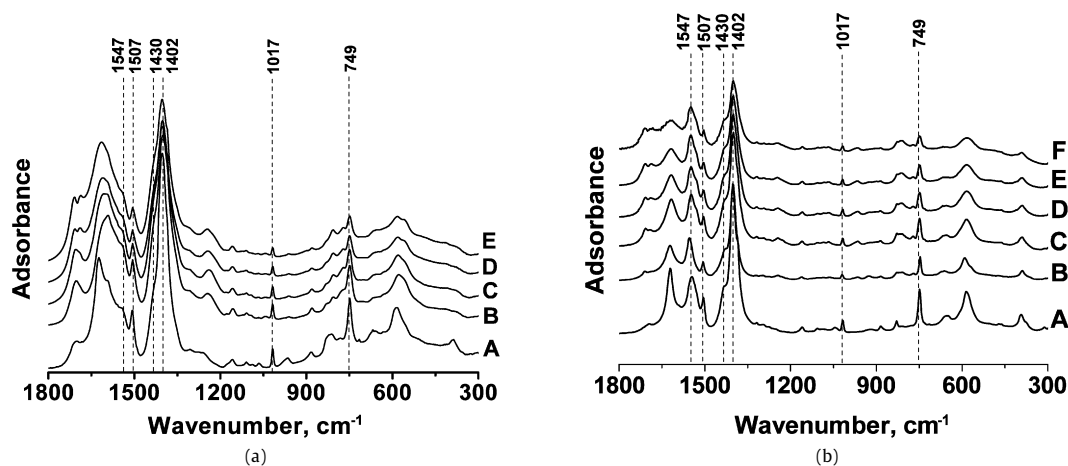


Fig. 13. FT-IR spectra of Ti-POM/MIL-101: (A) initial, (B)–(F) after 1–5 catalytic cycles of (a) α -pinene and (b) caryophyllene oxidation with H_2O_2 .

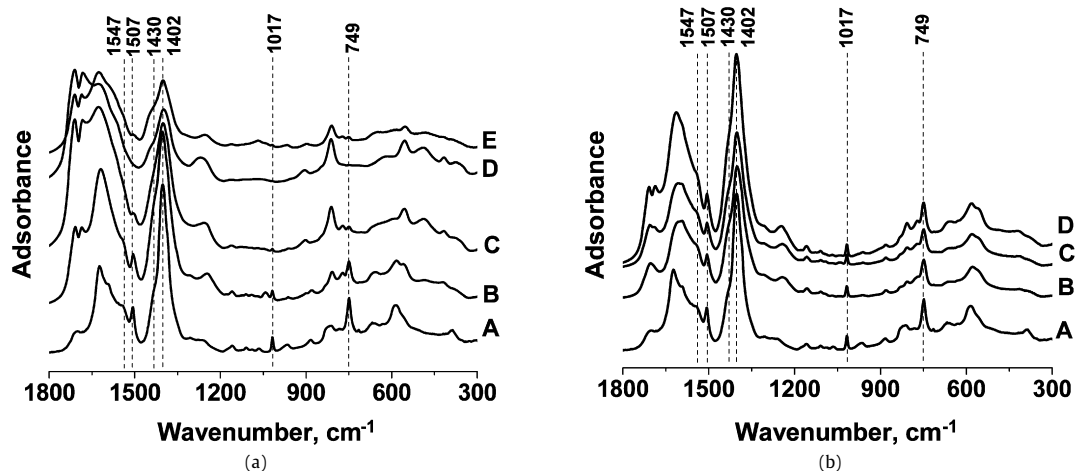


Fig. 14. FT-IR spectra of MIL-101: (A) initial, (B)–(E) after 1–4 treatments with (a) 0.4 M H_2O_2 at 70 °C and (b) 0.1 M H_2O_2 in MeCN at 70 °C for 6 h.

supramolecular structure. After both treatments with H_2O_2 , the catalyst lost its porous structure, as demonstrated by the textural data in Table 1.

4. Conclusion

Our findings demonstrate that Ti- and Co-monosubstituted Keggin POMs can be attached electrostatically to the surface of the

mesoporous zeotype coordination polymer MIL-101. The composite POM/MIL-101 materials demonstrate fairly good catalytic activity and selectivity in α -pinene allylic oxidation (81–84% verbenol/verbenone selectivity at 15–25% substrate conversion) and caryophyllene epoxidation (100% selectivity at 88% conversion) with green oxidants H_2O_2 (Ti-POM) and O_2 (Co-POM). The Co-POM/MIL-101 catalyst can be used repeatedly with no loss of activity and selectivity in oxidation with molecular oxygen. Reaction

conditions have a significant impact on the stability of the Ti-POM/MIL-101 catalyst when H₂O₂ is used as the oxidant. Under rather mild conditions (<50 °C, [H₂O₂] < 0.2 M), the Ti-POM/MIL-101 composite is rather stable, behaves as a true heterogeneous catalyst, does not undergo POM leaching, and can be recycled with no loss of catalytic properties. At higher H₂O₂ concentrations and higher temperatures, the MIL-101 matrix is destroyed, and the POM/MIL-101 catalyst undergoes deactivation.

Acknowledgments

The authors thank V. Utkin for identifying the oxidation products by GC/MS and E.V. Kulko for providing the particle size measurements. The research was partially supported by the Russian Foundation for Basic Research (RFBR-CNRS grant 05-03-34760).

References

- [1] R.A. Sheldon, M. Wallau, I.W.C.E. Arends, U. Schuchardt, *Acc. Chem. Res.* 31 (1998) 485.
- [2] I.W.C.E. Arends, R.A. Sheldon, *Appl. Catal. A Gen.* 212 (2001) 175.
- [3] J.S. Rafelt, J.H. Clark, *Catal. Today* 57 (2000) 33.
- [4] B. Notari, *Adv. Catal.* 41 (1996) 253.
- [5] G. Centi, S. Perathoner, in: I.T. Horvath (Ed.), *Encyclopedia of Catalysis*, vol. 6, Wiley-Interscience, NJ, 2003, p. 239.
- [6] M.T. Pope, *Heteropoly and Isopoly Oxometalates*, Springer-Verlag, Berlin, 1983.
- [7] J.B. Moffat, *Metal-Oxygen Clusters: The Surface and Catalytic Properties of Heteropoly Oxometalates*, Kluwer/Plenum, New York, 2001.
- [8] C.L. Hill, C.M. Prosser-McCartha, *Coord. Chem. Rev.* 143 (1995) 407.
- [9] N. Mizuno, M. Misino, *Chem. Rev.* 98 (1998) 199.
- [10] R. Neumann, *Prog. Inorg. Chem.* 47 (1998) 317.
- [11] J.E. Lyons, P.E. Ellis, V.A. Durante, *Stud. Surf. Sci. Catal.* 67 (1991) 99.
- [12] N. Mizuno, M. Tateishi, T. Hirose, M. Iwamoto, *Chem. Lett.* (1993) 2137.
- [13] N. Mizuno, T. Hirose, M. Iwamoto, *J. Mol. Catal.* 88 (1994) L125.
- [14] H. Weiner, R.G. Finke, *J. Am. Chem. Soc.* 121 (1999) 9831.
- [15] R. Neumann, M. Fahan, *J. Chem. Soc. Chem. Commun.* (1995) 2277.
- [16] M.T. Pope, in: A.G. Wedd (Ed.), *Comprehensive Coordination Chemistry II*, vol. 4, Elsevier, New York, 2004, p. 635.
- [17] R. Neumann, A.M. Khenkin, *Chem. Commun.* (2006) 2529.
- [18] C.L. Hill, in: A.G. Wedd (Ed.), *Comprehensive Coordination Chemistry II*, vol. 4, Elsevier, New York, 2004, p. 679.
- [19] J.M. Thomas, R. Raja, *Top. Catal.* 40 (2006) 3.
- [20] O.A. Kholdeeva, *Top. Catal.* 40 (2006) 229.
- [21] B.J.S. Johnson, A. Stein, *Inorg. Chem.* 40 (2001) 801.
- [22] R.J. Errington, S.S. Petkar, B.R. Horrocks, A. Houlton, L.H. Lie, S.N. Patole, *Angew. Chem. Int. Ed.* 44 (2005) 1254.
- [23] R. Neumann, H. Miller, *J. Chem. Soc. Chem. Commun.* (1995) 2277.
- [24] W. Kaleta, K. Nowinska, *Chem. Commun.* (2001) 535.
- [25] N.M. Okun, T.M. Anderson, C.L. Hill, *J. Am. Chem. Soc.* 125 (2003) 3194.
- [26] O.A. Kholdeeva, M.P. Vanina, M.N. Timofeeva, R.I. Maksimovskaya, T.A. Trubitsina, M.S. Melgunov, E.B. Burgina, J. Mrowiec-Bialon, A.B. Jarzelski, C.L. Hill, *J. Catal.* 226 (2004) 363.
- [27] M.V. Vasylyev, R. Neumann, *J. Am. Chem. Soc.* 126 (2004) 884.
- [28] J. Kasai, Y. Nakagawa, S. Uchida, K. Yamaguchi, N. Mizuno, *Chem. Eur. J.* 12 (2006) 4176.
- [29] G. Férey, C. Mellot-Draznieks, C. Serre, F. Millange, J. Dutour, S. Surble, I. Margiolaki, *Science* 309 (2005) 2040.
- [30] W.F. Erman, *Chemistry of the Monoterpenes: An Encyclopaedic Handbook*, Dekker, New York, 1985.
- [31] K. Bauer, D. Garbe, H. Surburg, *Common Fragrance and Flavor Materials*, Wiley-VCH, New York, 1997.
- [32] J.D. Connolly, R.A. Hill, *Dictionary of Terpenoids. Vol I: Mono- and Sesquiterpenoids*, Chapman & Hall, London, 1991.
- [33] *Rules and Regulations*, Food Drug Adm. 95 (38) (1973) 12913.
- [34] O.A. Kholdeeva, T.A. Trubitsina, M.N. Timofeeva, G.M. Maksimov, R.I. Maksimovskaya, V.A. Rogov, *J. Mol. Catal. A Chem.* 323 (2005) 173.
- [35] V.B. Fenelonov, V.N. Romannikov, A.Y. Derevyankin, *Micropor. Mesopor. Mater.* 28 (1999) 57.
- [36] D.W. Brown, A.J. Floyd, M. Sainsbury, *Organic Spectroscopy*, Wiley, New York, 1988.
- [37] E.F. Murphy, T. Mallat, A. Baiker, *Catal. Today* 57 (2000) 115.
- [38] N.V. Maksimchuk, M.S. Melgunov, J. Mrowiec-Bialon, A.B. Jarzelski, O.A. Kholdeeva, *J. Catal.* 235 (2005) 175.
- [39] N.V. Maksimchuk, M.S. Melgunov, Yu.A. Chesalov, J. Mrowiec-Bialon, A.B. Jarzelski, O.A. Kholdeeva, *J. Catal.* 246 (2007) 241.
- [40] P. McMorn, G. Roberts, G.J. Hutchings, *Catal. Lett.* 67 (2000) 203.
- [41] R.A. Sheldon, J.K. Kochi, *Metal-Catalyzed Oxidations of Organic Compounds*, Academic Press, New York, 1981.